

An Electrochemical Hydrogen Compression Model

Michael Bampaou^{a,b}, Kyriakos D. Panopoulos^{a,*}, Athanasios I. Papadopoulos^a,
Panos Seferlis^{a,b}, Spyros Voutetakis^a

^aChemical Process and Energy Resources Institute (CPERI), Centre for Research and Technology – Hellas (CERTH), Thessaloniki, Greece

^bDepartment of Mechanical Engineering, Aristotle University of Thessaloniki, Thessaloniki, Greece
panopoulos@certh.gr

The electrochemical hydrogen compressor (EHC) is a new system that can produce compressed purified H₂ out of a complex mixture of gases, which includes no moving parts and mechanical losses, and operates isothermally. The simulation of this system is the focus of this work in order to produce a zero-dimensional, steady-state EHC model for process design in commercial tools such as AspenPlus™. The model calculates the overall voltage by considering the Nernst voltage, the Ohmic losses, and the activation overpotentials. The required power and cooling load are thereafter evaluated, while taking into account the water management. The inclusion of the aforementioned phenomena results in an EHC system that considers several operating parameters and could be readily used for process integration.

1. Introduction

Electrochemical hydrogen compressor (EHC) combines hydrogen separation and purification in a compact equipment and is a device similar to a proton exchange membrane fuel cell (Chatrattanawet et al., 2016). A membrane acts as an electrolyte for protons exchange and is positioned between two catalysts containing electrodes, which are positioned between two porous gas diffusion layers (Millet and Grigoriev, 2014). Electrochemical compression is a one-stage isothermal process that requires about half of the adiabatic power required for a fixed compression ratio at constant temperature (Onda et al., 2007). In this work, an extensible EHC model is built with a detailed account of all the electrochemical equations governing voltage behaviour including the description of the water movements across the electrodes and membrane. The proposed model allows the investigation of various operating parameters and conditions, while it can also be easily integrated in flowsheets representing wider process systems. The steady-state zero-dimensional model is developed in AspenPlus™ using basic unit operation blocks to represent the main electrochemical operations, whereas voltage, current density and power requirements are externally modelled and implemented into the Fortran calculator block. Several operating parameters including back diffusion of hydrogen, cathode pressure, cooling requirements and water management are studied. The extent of water flooding issue and liquid water that should be removed are quantified to grasp the limitations of this application.

2. Working principle and basic modelling equations

2.1 Principle of operation

The principle of EHC operation is depicted in Figure 1. A humid gaseous feed containing H₂ and N₂ (or any other feed) is fed to the anode catalyst layer at low pressure. Once a potential difference is applied, the hydrogen oxidation reaction (HOR) occurs in the anode and H₂ is oxidised towards H⁺ protons. The protons travel through the membrane and are reduced to molecular H₂ by the hydrogen evolution reaction (HER) at elevated pressures. Eq(1) shows the relationship between the theoretical number of compressed hydrogen moles to the applied current:

$$n_{theoretical} = \frac{I}{2F} \quad (1)$$

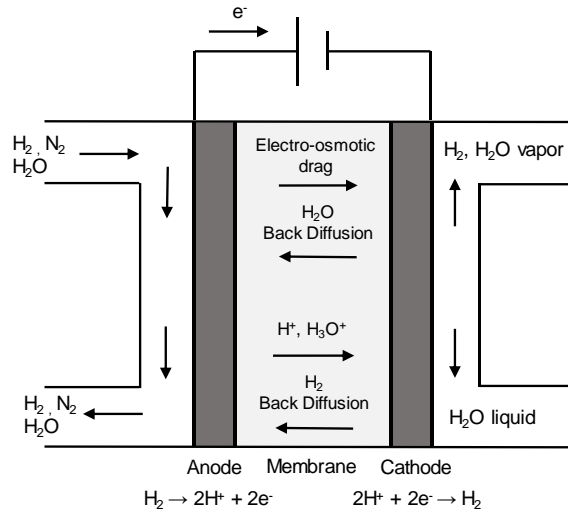


Figure 1: Principle of an electrochemical hydrogen compressor.

The theoretical cell voltage is determined by Nernst's equation. P_c refers to the H_2 partial pressure at cathode's exit and P_a to the H_2 partial pressure at anode's exit.

$$E_{Nernst} = \frac{RT}{2F} \ln \frac{P_c}{P_a} \quad (2)$$

The total cell voltage includes Ohmic and activation overpotentials. The conductivity of the membrane (σ) depends on the mean water content of the membrane (λ) (Springer et al., 1991):

$$\sigma_{303K} = 0.005139\lambda - 0.00326 \quad (3)$$

$$\sigma = \sigma_{303K} \cdot \exp \left[1268 \cdot \left(\frac{1}{303} - \frac{1}{T} \right) \right] \quad (4)$$

The measured mean water content of a Nafion® 117 membrane at temperatures 303 K (Springer, et al., 1991) and 353 K (Hinatsu, 1994) depend on water vapor activity α_w and the two experimental correlation are given as follows:

$$\lambda_{303} = 0.043 + 17.81\alpha_w - 39.85\alpha_w^2 + 36\alpha_w^3 \quad (5)$$

$$\lambda_{353} = 0.3 + 10.8\alpha_w - 16.0\alpha_w^2 + 14.1\alpha_w^3 \quad (6)$$

$$\alpha_w = x_w \frac{P}{P_{sat}} \quad (7)$$

As a result, Ohmic overpotentials are given by:

$$\eta_{ohmic} = \frac{\sigma}{L} j \quad (8)$$

where L is membrane thickness (= 0.02 cm for a fully hydrated Nafion® 117 membrane) (Ströbel et al., 2002). The activation polarisation refers to the energy barrier that should be overcome for an electrode reaction to occur. It is modelled by the Butler-Volmer type equations (Larminie and Dicks, 2001) and depends on the exchange current density of each electrode ($j_{oa,c}$).

$$\eta_{activation} = \frac{RT}{2a_{a,c}F} \ln \frac{j}{j_{oa,c}} \quad (9)$$

where $a_{a,c}$ is the anode/cathode charge transfer coefficient and is assumed to have a value of 0.5 (Neyerlin et al., 2007). Due to the lack of HOR and HER exchange current density values in the literature, the anode and cathode exchange currents are respectively based on PEMFC (Song et al., 2007) and PEM electrolyser (Harrison et al., 2006).

Eq(10) shows the total cell voltage that has to be applied as the sum of the Nernst potential plus the aforementioned overpotentials:

$$V_{cell} = E_{Nernst} + \eta_{ohmic} + \eta_{activation} = \frac{RT}{2F} \ln \frac{P_c}{P_a} + \frac{\sigma}{L} j + \frac{RT}{2a_{c,F}} \ln \frac{j}{j_{o,c}} + \frac{RT}{2a_{a,F}} \ln \frac{j}{j_{o,a}} \quad (10)$$

The required power to compress hydrogen at a given pressure is shown as follows:

$$P = V_{cell} I \quad (11)$$

The theoretical compressed H₂ flow rate that corresponds to the Faradaic current is reduced by hydrogen leaking and/or back-diffusion phenomenon. Hence, the actual compressed hydrogen is lower than the theoretical:

$$n_{back\ diffusion} = \alpha \frac{\Delta P}{L} A \quad (12)$$

$$I_{efficiency} = \frac{n_{theoretical} - n_{back\ diffusion}}{n_{theoretical}} \quad (13)$$

where ΔP represents the pressure difference between the anode and the cathode (bar) and α the hydrogen gas permeability coefficient of membrane (Kocha et al., 2006).

Water management is important to reduce proton resistance through the polymer electrolyte membrane. It is assumed that three different proton transport mechanisms are dominant in a hydrated membrane. These three different proton transport mechanisms are as follows: 1) direct transport from one Nafion® charged site to another, 2) the formation of hydronium complexes (H₃O⁺) and water usage as a means of transportation (vehicle mechanism), and 3) the use of water molecules as charged sites and transfer of protons from one site to another (hopping mechanism) (Jiao and Li, 2011).

Protons travelling from anode to cathode tend to drag water molecules. This flux is called electro-osmotic drag (EOD) and results in anode water depletion and membrane resistance increment.

$$J_{EOD} = n_d \frac{j}{F} \quad (14)$$

EOD is a function of the electro-osmotic drag coefficient (n_d), a parameter that describes the mean number of water molecules dragged through the membrane per travelling proton (Luo et al., 2010). In this work, n_d is considered as a linear relationship of membrane water content (Springer et al., 1991):

$$n_d = 2.5 \frac{\lambda}{22} \quad (15)$$

Due to the difference in water concentration between the anode and the cathode, water is travelling from the cathode to the anode or vice versa. This flux is called water back diffusion and is a function of the membrane water content (Springer et al., 1991):

$$J_{back\ diff.} = - \frac{\rho_M}{M_M} D_w \frac{d\lambda}{dz} \quad (16)$$

$$D_w = 4.17 \cdot 10^{-8} \lambda [161 \exp(-\lambda) + 1] \exp\left(\frac{-2346}{T}\right) \quad (17)$$

Hydraulic permeation refers to the water flux due to water pressure differences and is several orders of magnitude lower than EOD and water back diffusion. It is assumed to be negligible for modelling purposes. If the EOD is greater and the water cathode flux is such that it exceeds the saturation pressure of the hydrogen stream at a given temperature, liquid water accumulates in the cathode department. Flooded cathode is an undesired state that results in performance limitations, lower cell durability and unpredictable behaviour (Nguyen et al., 2011). On the other hand, if the water back diffusion is greater, the liquid water is accumulated on the anode side. Therefore, less water has to be fed with the feed gases. Water balance is attained under low current densities (< 0.1 A cm⁻²) and higher temperatures (> 343 K), where EOD and back diffusion fluxes are comparable. The water movements inside and outside of the membrane are depicted in Figures 1 and 2.

3. EHC modelling in AspenPlus™

The AspenPlus™ modelling methodology is shown in Figure 2. An example feed gas containing 50 % H₂ – 50 % N₂ is humidified to saturation with water vapour at a given temperature and introduced to the cell's anode. The energy balance accounts for the thermal sensible heat of the input as well as the compression power requirements, which are dissipated into cells (dashed lines).

For each set of calculations, an expected common temperature for the EHC operation was chosen. Any surplus of energy around the EHC model was evaluated as cooling load. Figure 2 shows that this cooling load depends also on the feed temperature, the temperature difference between humidifier temperature and operating temperature and the power required for the compression. The materials and energy balance around the EHC is at steady-state, while the process is considered as zero-dimensional and isothermal. Because of the electro-osmotic drag, the anode inlet gas mixture has to be kept saturated with water and at the same time no liquid

water should be present at the anode outlet. The membrane water activity is assumed 1 and the membrane is only hydrogen selective and gas permeation is negligible.

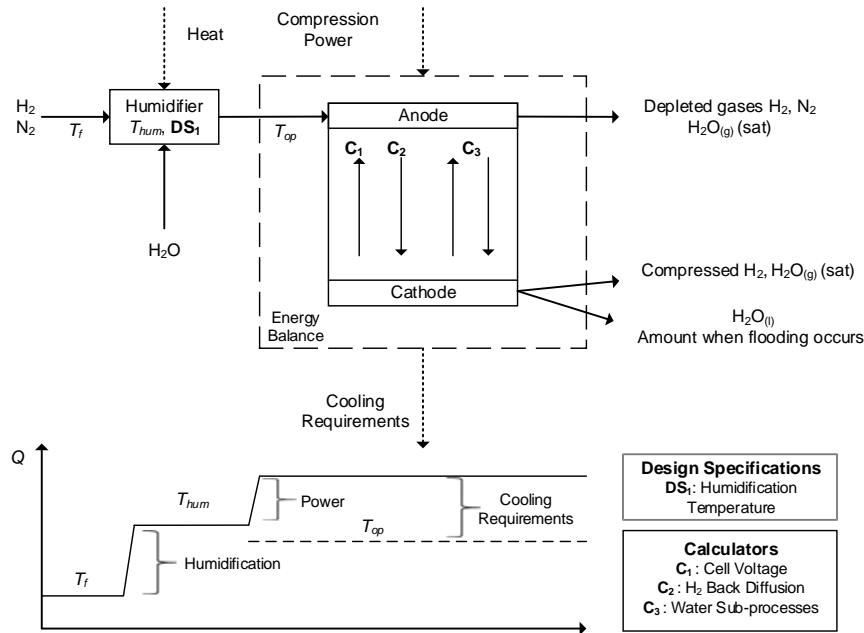


Figure 2: Schematic of the AspenPlus™ electrochemical hydrogen compression model and methodology of the cooling requirements calculation.

Table 1: Input Variables of the model.

Input Variables	Value	Reference
Active Surface, cm ²	50	Barbir and Görgün (2007), Casati et al. (2008)
Membrane	Nafion® 117	Grigoriev et al. (2011), Hao et al. (2016)
Wet Membrane Thickness, cm	0.2	Strobel et al. (2002)
Membrane density, g cm ⁻³	2	Zhou et al. (2006)
Membrane eq. weight, g mol ⁻¹	1,100	Mann et al. (2000)
Feed Composition	H ₂ – N ₂	Onda et al. (2007), Grigoriev et al. (2011), Hao et al. (2016), Onda et al. (2009)
Molar feed flow, mol s ⁻¹	0.0005	Assumption
Feed Temperature, K	298	Assumption
Water feed temperature, K	298	Assumption
Total feed pressure, bar	1	Assumption
Total cathode pressure, bar	1 – 150	Ströbel et al. (2002), Grigoriev et al. (2011)
Humidifier Temperature, K	333 – 358	Nguyen et al. (2011)
Operation temperature, K	313 – 343	Grigoriev et al. (2011), Rohland et al. (1998), Nguyen et al. (2011)

4. Results and discussions

Figure 3a shows the polarisation curves under different operating temperature and a cathode pressure of 10 bar. At lower current densities, cell voltages are similar because the temperature sensitive activation losses are negligible. However, as current densities are increased the overall cell voltages seem to decrease with increased temperatures. Figure 3b shows the polarisation curves under total cathode pressure: 1, 10, 50, and 150 bar at 343 K and the classification of the individual over-voltages at 10 bar. It is clear that the cell voltage increases with increased current density and cathode pressure resulting in higher cell voltages due to the Nernst potential.

The water balance and water sub-processes inside the membrane are illustrated in Figure 4a. If electro-osmotic drag diffusion is larger than water back diffusion, accumulation of water at the cathode occurs. The membrane needs to be adequately humidified to meet the process demands. Therefore, an external humidifier has to be

integrated into the system. The total water balance of the system is illustrated in Figure 4b. Higher humidifier temperatures result in higher cooling loads (Figure 5a). Figure 5b shows the overall energy efficiency of the system expressed as the lower heating value of H_2 (LHV, 244 kJ mol^{-1}) over the overall power consumption (the dotted line is the typical PEM electrolysis efficiency).

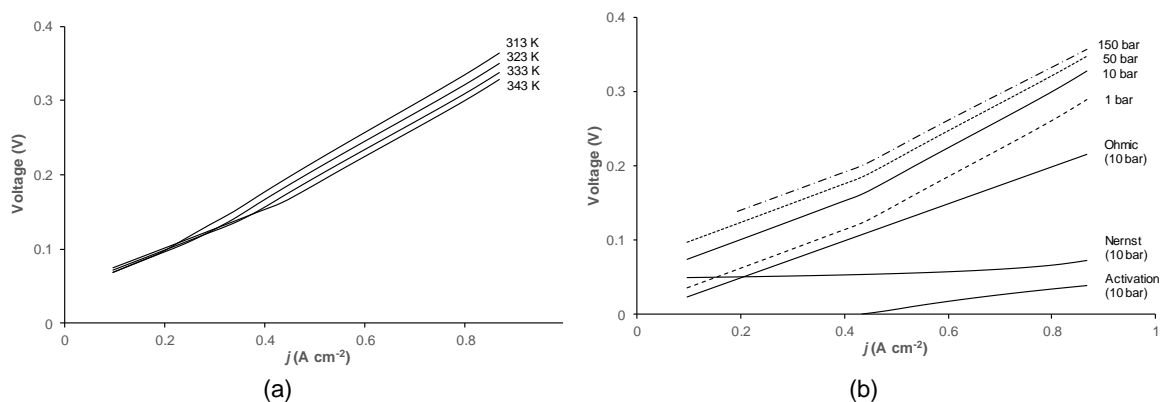


Figure 3: (a) Current-Voltage curves under different operating temperatures. (b) Polarisation Voltage curves at 343 K and cathode pressures from 10 – 150 bar

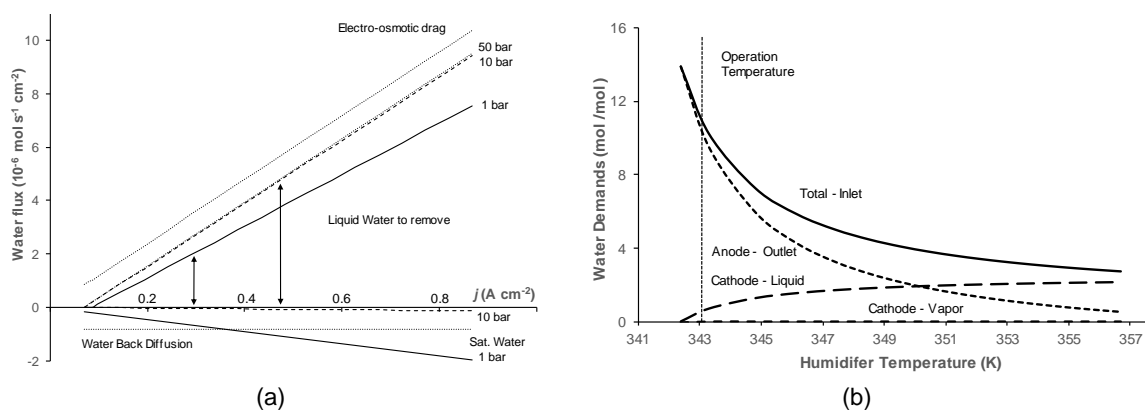


Figure 4: (a) Water sub-processes fluxes versus j . (b) Water balance outside the membrane and humidifier temperature expressed per H_2 mole.

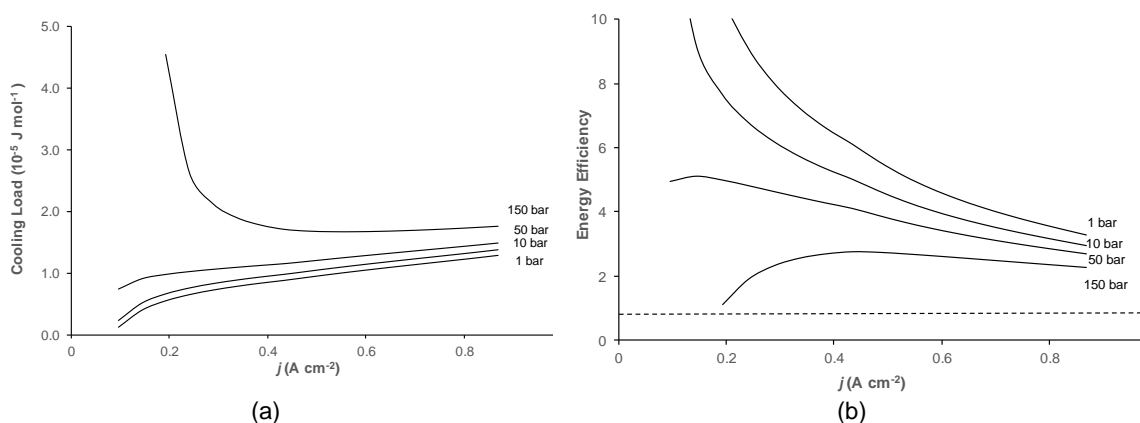


Figure 5: (a) Cooling requirements for EHC compressing 1 mole H_2 . (b) Energy efficiency of EHC versus employing water electrolysis producing fresh H_2 .

5. Conclusions

This study presents a detailed model of an electrochemical hydrogen compressor up to 343 K and 150 bar. Ohmic overvoltage is the main voltage loss, while the activation loss becomes apparent at higher current density. H₂ back diffusion is the major efficiency loss, especially at low current densities and increased cathode pressure, while at higher current densities, a subsidence of this phenomenon is observed. Water flooding can occur, which is attributed to water sub-processes inside and outside of the membrane.

References

- Barbir F., Görgün H., 2007, Electrochemical Hydrogen Pump for Recirculation of Hydrogen in a Fuel Cell Stack, *Journal of Applied Electrochemistry*, 37, 359–365.
- Casati C., Longhi P., Zanderighi L., Bianchi F., 2008, Some Fundamental Aspects in Electrochemical Hydrogen Purification/Compression, *Journal of Power Sources*, 180, 103–113.
- Chatrattanawet N., Hakhen T., Saebea D., Arpornwichanop A., 2016, Performance Analysis and Control Structure Design for Proton Exchange Membrane Fuel Cell, *Chemical Engineering Transactions*, 52, 997–1002.
- Grigoriev S.A., Shtatniy I.G., Millet P., Porembsky V.I., Fateev V.N., 2011, Description and Characterization of an Electrochemical Hydrogen Compressor/Concentrator Based on Solid Polymer Electrolyte Technology, *International Journal of Hydrogen Energy*, 36, 4148–4155.
- Hao Y.M., Nakajima H., Yoshizumi H., Inada A., Sasaki K., Ito K., 2016, Characterization of an Electrochemical Hydrogen Pump with Internal Humidifier and Dead-End Anode Channel, *International Journal of Hydrogen Energy*, 41, 13879–13887.
- Harrison K.W., Hernandez-Pacheco E., Mann M., Salehfar H., 2006, Semiempirical Model for Determining PEM Electrolyzer Stack Characteristics, *Journal of Fuel Cell Science and Technology*, 3, 220–223.
- Hinatsu J.T., Mizuhata M., Takenaka H., 1994, Water Uptake of Perfluorosulfonic Acid Membranes from Liquid Water and Water Vapor, *Journal of The Electrochemical Society*, 141, 1493–1498.
- Ibeh B., Gardner C., Ternan M., 2007, Separation of Hydrogen from a Hydrogen/Methane Mixture Using a PEM Fuel Cell, *International Journal of Hydrogen Energy*, 32, 908–914.
- Jiao K., Li X., 2011, Water Transport in Polymer Electrolyte Membrane Fuel Cells, *Progress in Energy and Combustion Science*, 37, 221–291.
- Kocha S.S., Yang J.D., Yi S.J., 2006, Characterization of Gas Crossover and Its Implications in PEM Fuel Cells, *AIChE Journal*, 52, 1916–1925.
- Larminie J., Dicks A., 2001, *Fuel Cell Systems Explained*, John Wiley & Sons Ltd., Chichester, UK.
- Luo Z., Chang Z., Zhang Y., Liu Z., Li J., 2010, Electro-osmotic Drag Coefficient and Proton Conductivity in Nafion® Membrane for PEMFC, *International Journal of Hydrogen Energy*, 35, 3120–3124.
- Mann R.F., Amphlett J.C., Hooper M.A.J., Jensen H.M., Peppley B.A., Roberge P.R., 2000, Development and Application of a Generalised Steady-State Electrochemical Model for a PEM Fuel Cell, *Journal of Power Sources*, 86, 173–180.
- Millet, P., Grigoriev, S.A., 2014, Electrochemical Characterization and Optimization of a PEM Water Electrolysis Stack for Hydrogen Generation, *Chemical Engineering Transactions*, 41, 7–12.
- Neyerlin K.C., Gu W., Jorne J., Gasteiger H.A., 2007, Study of the Exchange Current Density for the Hydrogen Oxidation and Evolution Reactions, *Journal of The Electrochemical Society*, 154, B631–B635.
- Nguyen M.T.D., Grigoriev S.A., Kalinnikov A.A., Filippov A.A., Millet P., Fateev V.N., 2011, Characterisation of a Electrochemical Hydrogen Pump Using Electrochemical Impedance Spectroscopy, *Journal of Applied Electrochemistry*, 41, 1033–1042.
- Onda K., Araki T., Ichihara K., Nagahama M., 2009, Treatment of Low Concentration Hydrogen by Electrochemical Pump or Proton Exchange Membrane Fuel Cell, *Journal of Power Sources* 188, 1–7.
- Onda K., Ichihara K., Nagahama M., Minamoto Y., Araki T., 2007, Separation and Compression Characteristics of Hydrogen by Use of Proton Exchange Membrane, *Journal of Power Sources* 164, 1–8.
- Rohland B., Eberle K., Strobel R., Scholta J., Garche J., 1998, Electrochemical Hydrogen Compressor, *Electrochimica Acta*, 43, 3841–3846.
- Song C., Tang Y., Zhang J.L., Zhang J., Wang H., Shen J., McDermid S., Li J., Kozak P., 2007, PEM Fuel Cell Reaction Kinetics in the Temperature Range of 23–120 °C, *Electrochimica Acta*, 52, 2552–2561.
- Springer T.E., Zawodzinski T.A., Gottesfeld S., 1991, Polymer Electrolyte Fuel Cell Model, *Journal of the Electrochemical Society*, 138, 2334–2342.
- Ströbel R., Oszcipok M., Fasil M., Rohland B., Jörissen L., Garche J., 2002, The Compression of Hydrogen in an Electrochemical Cell Based on a PE Fuel Cell Design, *Journal of Power Sources*, 105, 208–215.
- Zhou B., Huang W., Zong Y., Sobiesiak A., 2006, Water and Pressure Effects on a Single PEM Fuel Cell, *Journal of Power Sources*, 155, 190–202.